Supporting Information

Spontaneous Tl(I)-to-Tl(III) Oxidation in Dynamic Heterobimetallic Hg(II)/Tl(I) Porphyrin Complexes

Victoria Ndoyom,[a] Luca Fusaro,[b] Thierry Roisnel,[a] Stéphane Le Gac*[a] and Bernard Boitrel*[a]

(a) UMR CNRS 6226, Institut des Sciences Chimiques de Rennes, Université de Rennes 1, 263 avenue du Général Leclerc, 35042 Rennes cedex, France.

E-mail : stephane.legac@univ-rennes1.fr; bernard.boitrel@univ-rennes1.fr

(b) Unité de Chimie des Nanomatériaux (CNANO), Université de Namur, 61 rue de Bruxelles, B-5000 Namur, Belgium.

Content:

Experimental Section

Experimental Section

General

All of the NMR experiments were conducted in 5 mm standard NMR tubes. ^{1}H NMR spectra were recorded at 400 or 500 MHz. Chemical shifts are expressed in parts per million, and traces of residual solvents were used as internal standards. All of the ^{1}H NMR signals were assigned using 2D NMR experiments (COSY, HSQC). Compounds **1**[1] and **2**[2] were prepared as previously described. All of the chemicals were commercial products and used as received. ***Caution! Thallium salts are highly toxic and should be handled with care.***

^{205}Tl Heteronuclear NMR experiments

Natural abundance ^{205}Tl and ^{1}H NMR spectra were recorded at 25° C, on a Varian VNMR System spectrometer operating at 9.4 T (230.9 and 399.9 MHz, respectively) equipped with three channels (one high band and two low band) and temperature regulation, using a modified 5 mm switchable probe. The spectra of Tl(I) were recorded using the following acquisition parameters: spectral width of about 832 ppm (192 kHz), 0.06 s relaxation delay, 17 µs (90°) excitation pulse, 5 ms acquisition time and a number of transients ranging between 6.8×10^{3} and 8.7×10^{5}. The spectra of Tl(III) were recorded using the following acquisition parameters: spectral width of about 832 ppm (192 kHz), 4.9 s relaxation delay, 90° excitation pulse, 0.1 s acquisition time and a number of transients ranging between 3.0×10^{2} and 1.2×10^{4}. The spectra were recorded lock-on without sample spinning. The processing comprised correction of the Free Induction Decay (FID) by backward linear prediction, exponential multiplication with a line broadening factor of 200 Hz, zero filling, Fourier transform, zero-order phase correction, and baseline correction. The chemical shift scale was calibrated at 25°C with respect to an aqueous $TlNO_3$ solution at infinite dilution (0 ppm).[3]

General procedure for the formation of complexes $\mathbf{1}^{Hg}$, $\mathbf{1}^{Hg}_{Tl(I)}$, $\mathbf{2}^{Hg}$ and $\mathbf{2}^{Hg}_{Tl(I)}$

The complexes $\mathbf{1}^{Hg}$ and $\mathbf{2}^{Hg}$ were prepared by mixing the free base porphyrins **1** or **2** (2.38 µmol, 1 equiv.) in 500 µL of 9:1 mixture of $CDCl_3/CD_3OD$, 4 µL of DIPEA (23.8 µmol, 10 equiv.) and 40 µL (2.38 µmol, 1 equiv.) of a stock solution of $Hg(OAc)_2$ (9.5 mg in 500 µL of 9:1 $CDCl_3/CD_3OD$). In the case of $\mathbf{2}^{Hg}$,[4] the formation of a bimetallic complex (**$2Hg_2$**, structure in Figure S14) is also observed. Then the bimetallic complexes $\mathbf{1}^{Hg}_{Tl(I)}$ or $\mathbf{2}^{Hg}_{Tl(I)}$ were formed by adding 30 µL (2.38 µmol, 1 equiv.) of a stock solution of TlOAc (10.5 mg in 500 µL of 9:1 $CDCl_3/CD_3OD$). The ^{1}H NMR spectrum recorded at 298 K showed the quasi-quantitative formation of the desired complexes.

Characterization of complexes $\mathbf{1}^{Hg}$, $\mathbf{2}^{Hg}$, $\mathbf{1}^{Hg}_{Tl(I)}$, $\mathbf{1}^{Tl(III)}$ and $\mathbf{2}^{Hg}_{Tl(I)}$

$\mathbf{1}^{Hg}$: ^{1}H NMR (400 MHz, $CDCl_3/CD_3OD$ 9:1, DIPEA, 298 K) : δ 8.94 (d, J = 8.2 Hz, 2H, HAr_{meso}), 8.93 (d, J = 4.5 Hz, 2H, $H_{\beta pyr}$), 8.76 (d, J = 4.5 Hz, 2H, $H_{\beta pyr}$), 8.73 (d, J = 4.5 Hz, 2H, $H_{\beta pyr}$), 8.62 (d, J = 4.5 Hz, 2H, $H_{\beta pyr}$), 7.90 (d, J = 7.5 Hz, 2H, HAr_{meso}), 7.79 (t, J = 8.0 Hz, 2H, HAr_{meso}), 7.52 (s, 1H, $HAr_{m\text{-}OMe}$), 7.44 (t, J = 8.0 Hz, 2H, HAr_{meso}), 7.43 (d, J = 7.5 Hz, 2H, HAr_{meso}), 7.38 (s, 1H, $HAr_{m\text{-}OMe}$), 7.31 (s, 1H, $HAr_{m\text{-}OMe}$), 6.98 (s, 1H, $HAr_{m\text{-}OMe}$), 6.85 (t, J = 7.8 Hz, 2H, HAr_{strap}), 6.82 (t, J = 2.3 Hz, 1H, $HAr_{m\text{-}OMe}$), 6.76 (s, 1H, $HAr_{m\text{-}OMe}$), 6.63 (d, J = 7.5 Hz, 2H, HAr_{strap}), 5.19 (s, 2H, HAr_{strap}), 3.91 (s, 3H, CH_3), 3.90 (s, 3H, CH_3), 3.88 (s, 3H, CH_3), 3.78 (s, 3H, CH_3), 1.80 (m, 2H, $CH_{2,benz}$), 1.09 (m, 2H, $CH_{2,benz}$), 0.82 (m, 1H, CHCO). 2D HSQC NMR $\delta(^{13}C)$: 134.3 (2C), 133.4 (2C), 132.0 (2C), 131.6 (2C), 131.3 (2C), 130.3 (2C), 129.3 (2C),

---

[1] S. Le Gac, B. Najjari, L. Fusaro, T. Roisnel, V. Dorcet, M. Luhmer, E. Furet, J.-F. Halet and B. Boitrel, *Chem. Commun.,* 2012, **48**, 3724-3726.

[2] Z. Halime, M. Lachkar, T. Roisnel, E. Furet, J.-F. Halet and B. Boitrel, *Angew. Chem. Int. Ed.,* 2007, **46**, 5120-5124.

[3] R. W. Briggs, K. R. Metz and J. F. Hinton, *Journal of Solution Chemistry,* 1979, **8**, 479-487.

[4] N. Motreff, S. Le Gac, M. Luhmer, E. Furet, J.-F. Halet, T. Roisnel and B. Boitrel, *Angew. Chem. Int. Ed.,* 2011, **50**, 1560-1564.

128.1 (2C), 126.0 (2C), 125.4 (2C), 122.6 (2C), 119.0 (2C), 115.0, 114.9, 114.4, 114.1, 99.7, 99.0, 55.5 (4C), 39.9 (2C) ppm. HRMS (ESI) : m/z calculated 1255.33237 $[M]^-$ for $C_{66}H_{49}N_6O_8{}^{202}Hg$, found 1255.3326 (0 ppm).

2^{Hg}: ^{1}H NMR (400 MHz, $CDCl_3/CD_3OD$ 9:1, DIPEA, 298 K) : δ 8.92 (d, J = 8.4 Hz, 2H, HAr_{meso}), 8.85 (d, J = 7.9 Hz, 2H, HAr_{meso}), 8.79 (d, J = 4.5 Hz, 2H, $H_{\beta pyr}$), 8.75 (s, 2H, $H_{\beta pyr}$), 8.70 (d, J = 4.5 Hz, 2H, $H_{\beta pyr}$), 8.68 (s, 2H, $H_{\beta pyr}$), 8.24 (d, J = 7.4 Hz, 2H, HAr_{meso}), 8.00 (d, J = 7.5 Hz, 2H, HAr_{meso}), 7.80 – 7.73 (m, 4H, HAr_{meso}), 7.48 – 7.42 (m, 4H, HAr_{meso}), 7.39 (d, J = 7.5 Hz, 2H, HAr_{strap}), 7.28 (d, J = 7.5 Hz, 2H, HAr_{strap}), 6.88 (t, J = 7.5 Hz, 2H, HAr_{strap}), 6.78 (t, J = 7.7 Hz, 2H, HAr_{strap}), 6.74 (d, J = 8 Hz, 2H, HAr_{strap}), 6.61 (d, J = 7.6 Hz, 2H, HAr_{strap}), 5.32 (s, 2H, HAr_{strap}), 5.02 (s, 2H, HAr_{strap}), 1.53 (m, 6H, CH_2benz + CHCO), 1.28 (m, 4H, CH_2benz). HRMS (ESI) : m/z calculated 1479.36686 for $[M\text{-}H+Na]^-$ $C_{80}H_{54}N_8O_8Na^{202}Hg$, found 1479.3681 (0 ppm).

1$^{Hg}_{Tl(I)}$: ^{1}H NMR (500 MHz, $CDCl_3/CD_3OD$ 9:1, DIPEA, 298 K): δ 9.16 (d, J = 4.5 Hz, 2H, $H_{\beta pyr}$), 9.00 (d, J = 4.5 Hz, 2H, $H_{\beta pyr}$), 8.99 (d, J = 4.5 Hz, 2H, $H_{\beta pyr}$), 8.94 (d, J = 7.4 Hz, 2H, HAr_{meso}), 8.86 (d, J = 4.6 Hz, 2H, $H_{\beta pyr}$), 7.99 (d, J = 7.4 Hz, 2H, HAr_{meso}), 7.90 (s, 1H, $HAr_{m\text{-}OMe}$), 7.84 (td, J = 7.9, 1.6 Hz, 2H, HAr_{meso}), 7.50 (td, J = 8.8, 1.6 Hz, 2H, HAr_{meso}), 7.49 (s, 1H, $HAr_{m\text{-}OMe}$), 7.41 (d, J = 8.0 Hz, 2H, HAr_{strap}), 7.36 (s, 1H, $HAr_{m\text{-}OMe}$), 7.29 (s, 1H, $HAr_{m\text{-}OMe}$), 7.25 (s, 1H, $HAr_{m\text{-}OMe}$), 6.89 (t, J = 7.6 Hz, 2H, HAr_{strap}), 6.87 (t, J = 2.2 Hz, 1H, $HAr_{m\text{-}OMe}$), 6.78 (t, J = 2.2 Hz, 1H, $HAr_{m\text{-}OMe}$), 6.61 (d, J = 7.6 Hz, 2H, HAr_{strap}), 5.10 (s, 2H, HAr_{strap}), 3.95 (s, 3H, CH_3), 3.87(3) (s, 3H, CH_3), 3.87(1) (s, 3H, CH_3), 3.77 (s, 3H, CH_3), 1.95 (d, J = 12.2 Hz, 2H, $CH_{2,benz}$), 1.22 (m, 2H, $CH_{2,benz}$), 0.92 (m, 1H, CHCO). ^{205}Tl NMR (231 MHz, $CDCl_3/CD_3OD$ 9:1, DIPEA, 298 K): δ 1114 ppm. 2D HSQC NMR $\delta(^{13}C)$: 134.8 (2C), 134.4 (2C), 133.6 (2C), 132.6 (2C), 131.9 (2C), 131.5 (2C), 129.5 (2C), 128.3 (2C), 126.2 (2C), 124.3 (2C), 122.8 (2C), 120.3 (2C), 114.3, 114.2, 114.0, 113.7, 100.1, 99.8, 55.4 (4C), 40.3 (2C) ppm. UV-vis ($CHCl_3/CH_3OH$ 9:1, DIPEA): λ 461, 586, 632 nm. HRMS (ESI) : m/z calculated 1459.29896 for $[M\text{-}H]^-$ $C_{66}H_{48}N_6O_8{}^{202}Hg^{205}Tl$, found 1459.2999 (1 ppm) (**1**$^{Hg}_{Tl(I)}$ is observed with a weak intensity, ca. 5-10% vs. the mononuclear Hg(II) complex **1**^{Hg}, likely as a result of a demetallation process occurring during the mass analysis).

1$^{Tl(III)}$: ^{1}H NMR (500 MHz, $CDCl_3/CD_3OD$ 9:1, DIPEA, 298 K): δ 9.15 (dd, J = 63, 4.7 Hz, 2H, $H_{\beta pyr}$), 8.99 (dd, J = 68, 4.7 Hz, 2H, $H_{\beta pyr}$), 8.96 (dd, J = 63, 4.7 Hz, 2H, $H_{\beta pyr}$), 8.85 (d, J = 8.5 Hz, 2H, HAr_{meso}), 8.83 (dd, J = 68, 4.7 Hz, 2H, $H_{\beta pyr}$), 7.94 (d, J = 7.4 Hz, 2H, HAr_{meso}), 7.86 (td, J = 8.2, 1.6 Hz, 2H, HAr_{meso}), 7.51 (t, J = 7.2 Hz, 2H, HAr_{meso}), 7.49 (d, J = 7.2 Hz, 2H, HAr_{strap}), 7.43 (s, 1H, $HAr_{m\text{-}OMe}$), 7.37 (s, 1H, $HAr_{m\text{-}OMe}$), 7.10 (s, 1H, $HAr_{m\text{-}OMe}$), 6.91 (t, J = 7.7 Hz, 2H, HAr_{strap}), 6.86 (t, J = 2.3 Hz, 1H, $HAr_{m\text{-}OMe}$), 6.78 (t, J = 2.3 Hz, 1H, $HAr_{m\text{-}OMe}$), 6.52 (d, J = 7.5 Hz, 2H HAr_{strap}), 5.12 (s, 2H HAr_{strap}), 3.93 (s, 3H, CH_3), 3.89 (s, 3H, CH_3), 3.83 (s, 3H, CH_3), 3.82 (s, 3H, CH_3), 1.64 (dd, J = 26.5, 12.9 Hz, 2H, $CH_{2,benz}$), 1.19 – 1.07 (m, 2H, $CH_{2,benz}$), 0.72 (m, 1H, CHCO). ^{205}Tl NMR (231 MHz, $CDCl_3/CD_3OD$ 9:1, DIPEA, 298 K): δ 2558 ppm. 2D HSQC NMR $\delta(^{13}C)$: 133.9 (2C), 133.6 (2C), 133.0 (2C), 132.0 (2C), 131.8 (2C), 130.9 (2C), 129.8 (2C), 128.4 (2C), 126.1 (2C), 123.8 (2C), 123.1 (2C), 120.6 (2C), 114.9, 114.0, 113.8, 113.6, 100.3, 99.9, 55.5 (4C) 39.7 (2C) ppm. UV-vis ($CHCl_3/CH_3OH$ 9:1, DIPEA): λ (ε, $M^{-1}.cm^{-1}$) 436 (3.3×10^6), 564 (1.7×10^4), 605 (4.9×10^3) nm. HRMS (ESI) : m/z calculated 1257.32832 for $[M\text{-}H]^-$ $C_{66}H_{48}N_6O_8{}^{205}Tl$, found 1257.3288 (0 ppm).

2$^{Hg}_{Tl(I)}$: ^{1}H NMR (500 MHz, $CDCl_3/CD_3OD$ 9:1, DIPEA, 298 K): δ 9.01 (s, 2H, $H_{\beta pyr}$), 8.90 (d, J = 4.5 Hz, 2H, $H_{\beta pyr}$), 8.86 (d, J = 4.5 Hz, 2H, $H_{\beta pyr}$), 8.75 (s, 2H, $H_{\beta pyr}$), 8.64 (d, J = 8.4 Hz, 2H, HAr_{meso}), 8.54 (d, J = 8.4 Hz, 2H, HAr_{meso}), 8.18 (d, J = 7.4 Hz, 2H, HAr_{meso}), 8.05 (d, J = 7.4 Hz, 2H, HAr_{meso}), 7.83 (td, J = 8.3 1.6 Hz, 2H, HAr_{meso}), 7.77 (td, J = 8.0, 1.6 Hz, 2H, HAr_{meso}), 7.58 (td, J = 7.6, 1.0 Hz, 2H, HAr_{meso}), 7.50 (td, J = 7.6, 1.0 Hz, 2H, HAr_{meso}), 7.25 (d, J = 7.7 Hz, 2H, HAr_{strap}), 7.22 (d, J = 7.7 Hz, 2H, HAr_{strap}), 6.84 (t, J = 7.5 Hz, 2H, HAr_{strap}), 6.83 (t, J = 7.5 Hz, 2H, HAr_{strap}), 6.63 (d, J = 7.7 Hz, 2H, HAr_{strap}), 6.62 (d, J = 7.7 Hz, 2H, HAr_{strap}), 5.44 (s, 2H, HAr_{strap}), 5.33 (s, 2H, HAr_{strap}), 1.89 (m, 4H, $CH_{2,benz}$), 1.44 (m, 4H, $CH_{2,benz}$),

1.16 (m, 2H, CHCO). ^{205}Tl NMR (231 MHz, $CDCl_3/CD_3OD$ 9:1, DIPEA, 298 K): δ 895 ppm. 2D HSQC NMR $\delta(^{13}C)$: 135.3 (2C), 134.9 (2C), 133.5 (2C), 133.3 (2C), 132.7 (2C), 132.6 (2C), 131.5 (4C), 129.3 (2C), 129.2 (2C), 128.0 (4C), 125.6 (4C), 124.9 (2C), 124.7 (2C), 123.5 (4C), 122.0 (2C), 121.9 (2C), 52.9 (2C), 39.4 (4C) ppm. UV-vis ($CHCl_3/CH_3OH$ 9:1, DIPEA): λ 464, 588, 635 nm. HRMS (ESI) : m/z calculated 1661.35205 for $[M]^-$ $C_{80}H_{54}N_8O_8{}^{202}Hg^{205}Tl$, found 1661.3527 (0 ppm).

Crystal data for complex $1^{Tl(III)}$

$C_{66}H_{49}N_6O_8Tl$; M = 1258.48. APEXII, Bruker-AXS diffractometer, Mo-Kα radiation (λ = 0.71073 Å), T = 150(2) K; Monoclinic $P\ 1\ 2_1/n\ 1$, a = 14.4652(8), b = 17.5010(10), c = 23.3205(14) Å, β = 91.874(2) °, V = 5900.6(6) $Å^3$. Z = 4, d = 1.417 $g.cm^{-3}$, μ = 2.798 mm^{-1}. The structure was solved by direct methods using the *SIR97* program,[5] and then refined with full-matrix least-square methods based on F^2 (*SHELXL-97*).[6] The contribution of the disordered solvents to the calculated structure factors was estimated following the *BYPASS* algorithm,[7] implemented as the *SQUEEZE* option in *PLATON*.[8] A new data set, free of solvent contribution, was then used in the final refinement. All non-hydrogen atoms were refined with anisotropic atomic displacement parameters. H atoms were finally included in their calculated positions. A final refinement on F^2 with 13504 unique intensities and 734 parameters converged at $\omega R(F^2)$ = 0.1188 ($R(F)$ = 0.0515) for 8250 observed reflections with $I > 2\sigma(I)$. CCDC 1422859.

[5] A. Altomare, M. C. Burla, M. Camalli, G. Cascarano, C. Giacovazzo, A. Guagliardi, A. G. G. Moliterni, G. Polidori and R. Spagna, *J. Appl. Crystallogr.,* 1999, **32**, 115-119.
[6] G. M. Sheldrick, *Acta Crystallogr.,* 2008, **A64**, 112-122.
[7] P. van der Sluis and A. L. Spek, *Acta Crystallogr.,* 1990, **A46**, 194-201.
[8] A. L. Spek, *J. Appl. Crystallogr.,* 2003, **36**, 7-13.

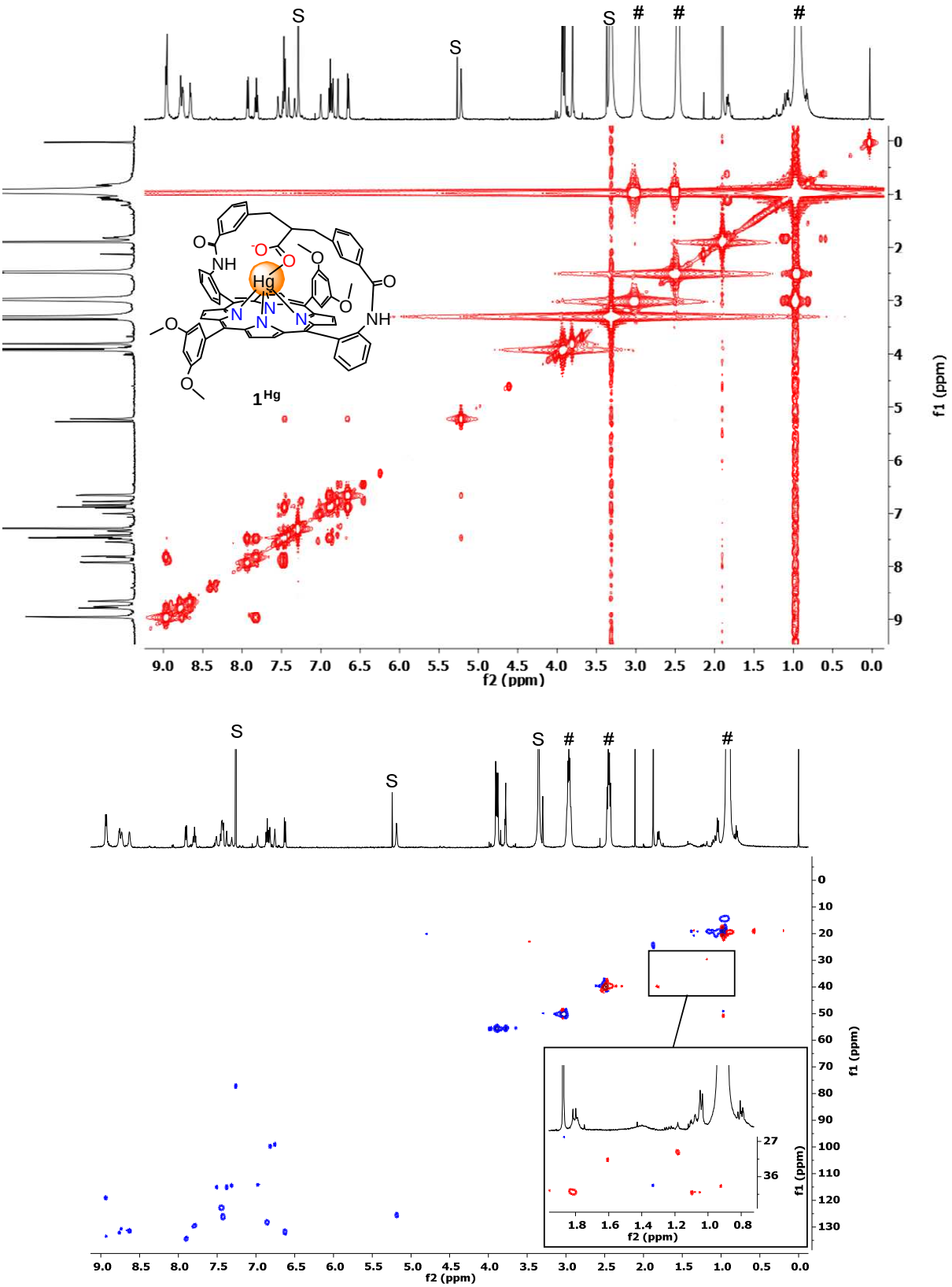

Figure S1. 2D COSY (top) and HSQC (bottom) NMR spectra of **1**^{Hg} in $CDCl_3/CD_3OD$ (9:1) with 10 equiv. of DIPEA at 298 K, (400 MHz). S = solvents, # = DIPEA.

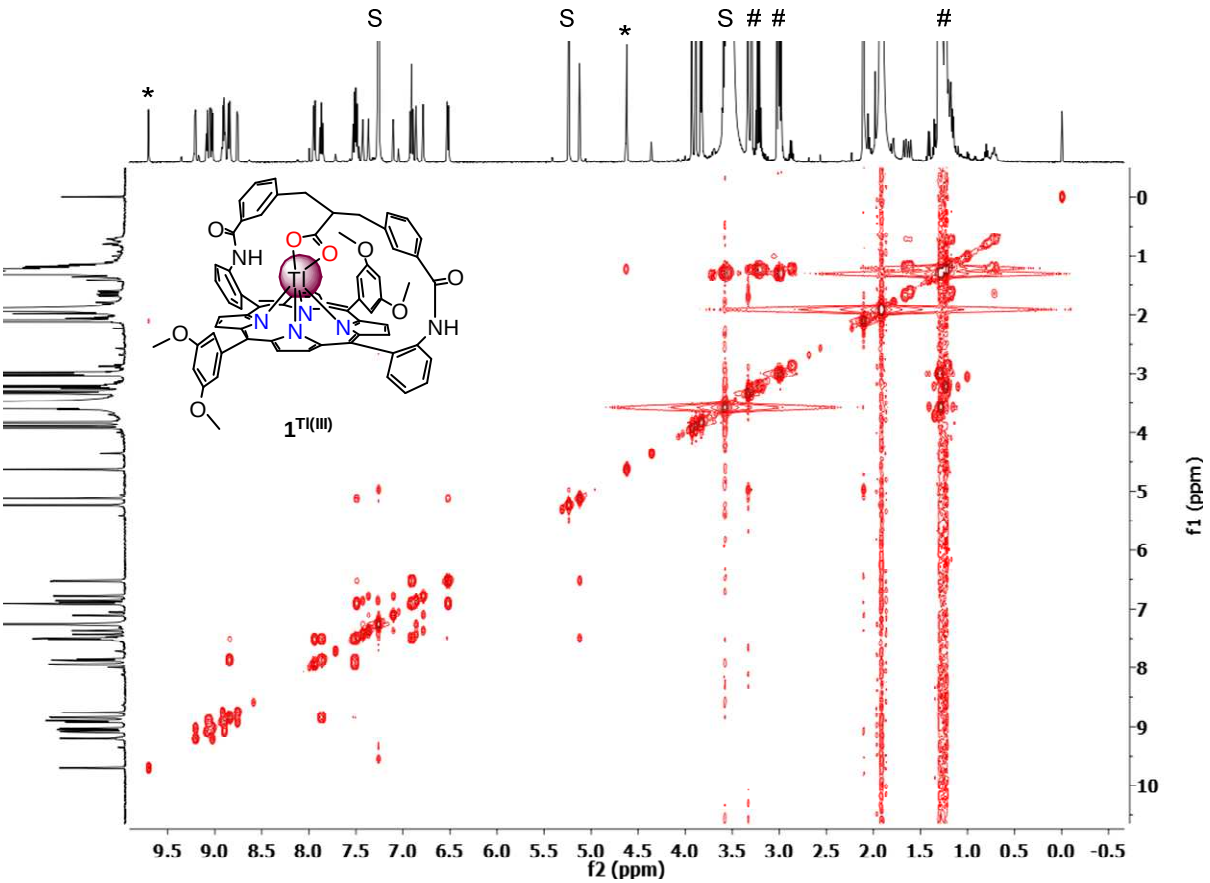

Figure S2. 2D COSY NMR spectrum of $\mathbf{1}^{Tl(III)}$ in $CDCl_3/CD_3OD$ (9:1) with 10 equiv. of DIPEA at 298 K (400 MHz). S = solvents, * = impurities, # = DIPEA.

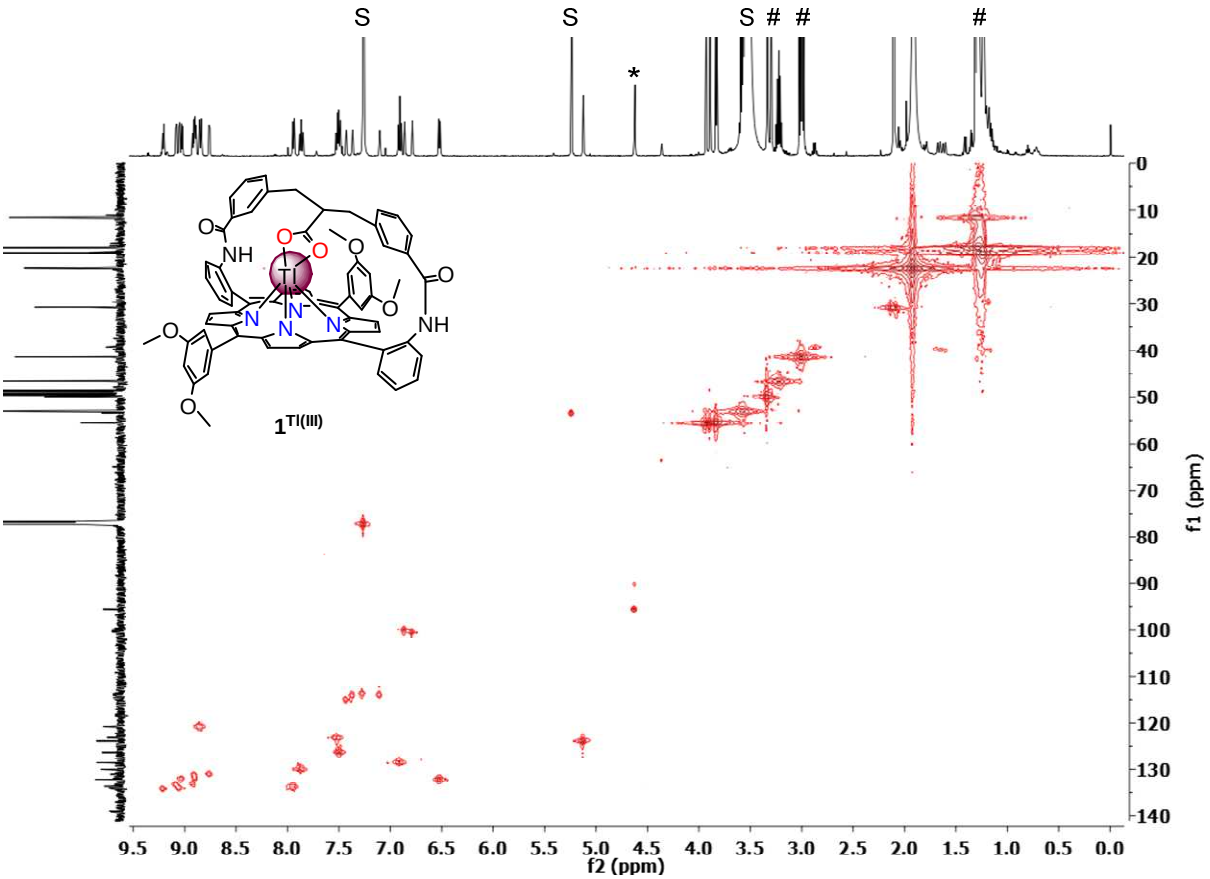

Figure S3. 2D HSQC NMR spectrum of $\mathbf{1}^{Tl(III)}$ in $CDCl_3/CD_3OD$ (9:1) with 10 equiv. of DIPEA at 298 K (500 MHz). S = solvents, * = impurity, # = DIPEA.

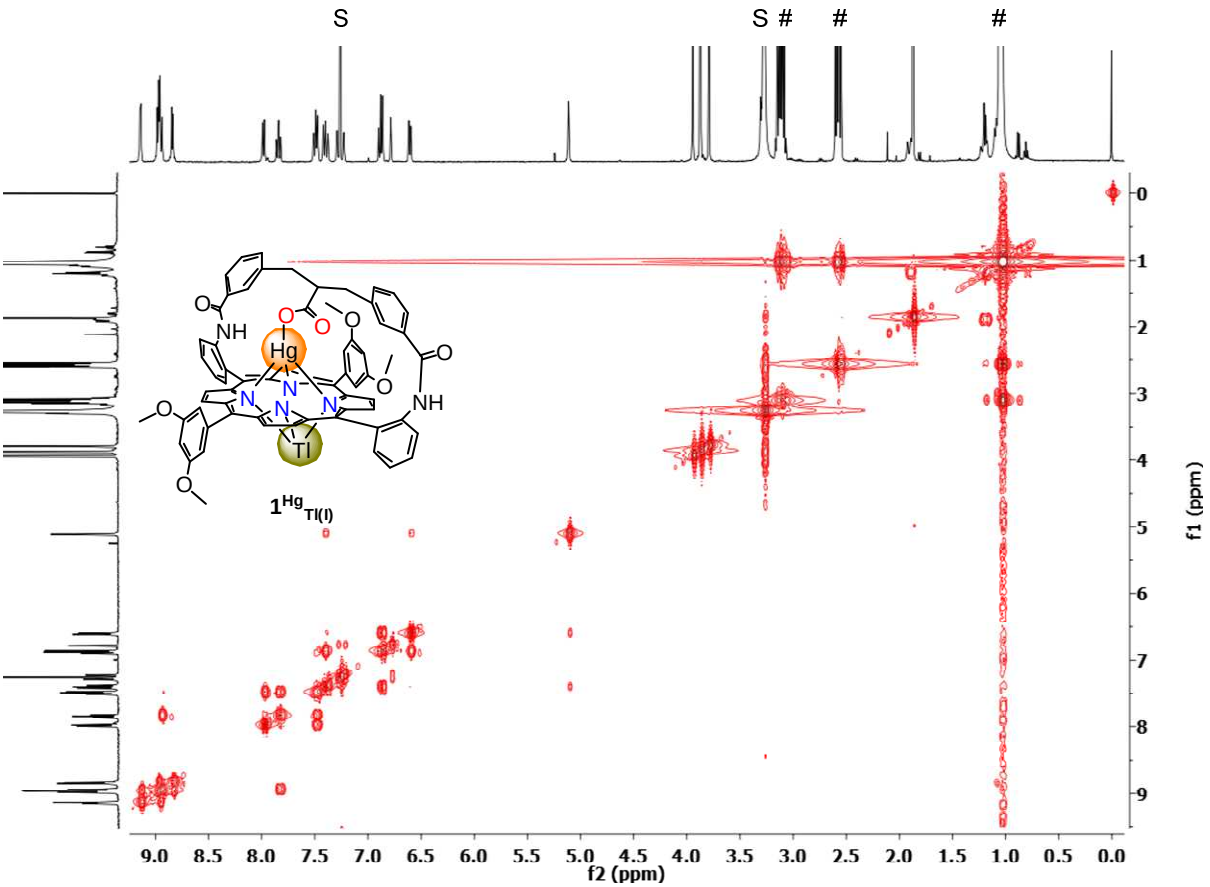

Figure S4. 2D COSY NMR spectrum of $\mathbf{1}^{Hg}_{Tl(I)}$ in $CDCl_3/CD_3OD$ (9:1) with 10 equiv. of DIPEA at 298 K (400 MHz). S = solvents, # = DIPEA.

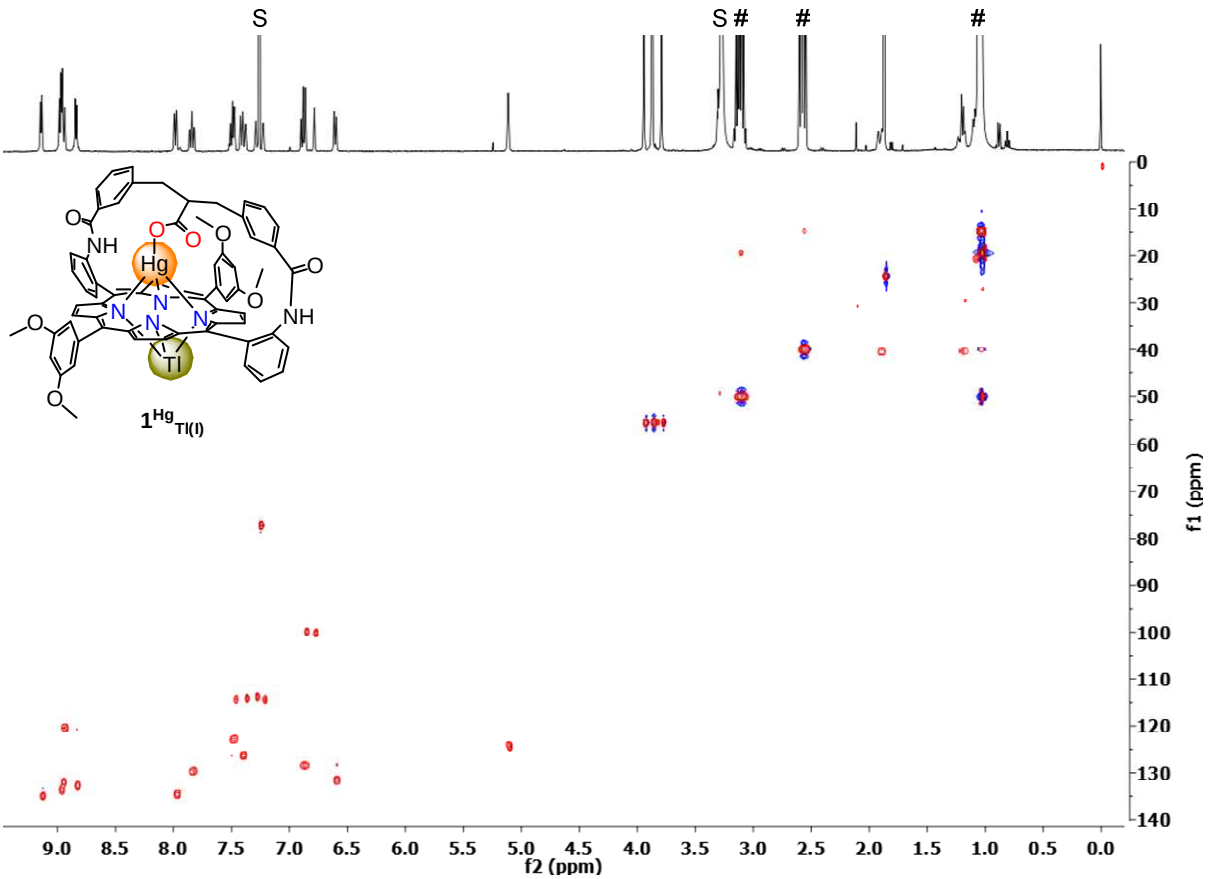

Figure S5. 2D HSQC NMR spectrum of $\mathbf{1}^{Hg}_{Tl(I)}$ in $CDCl_3/CD_3OD$ (9:1) with 10 equiv. of DIPEA at 298 K (400 MHz). S = solvents, # = DIPEA.

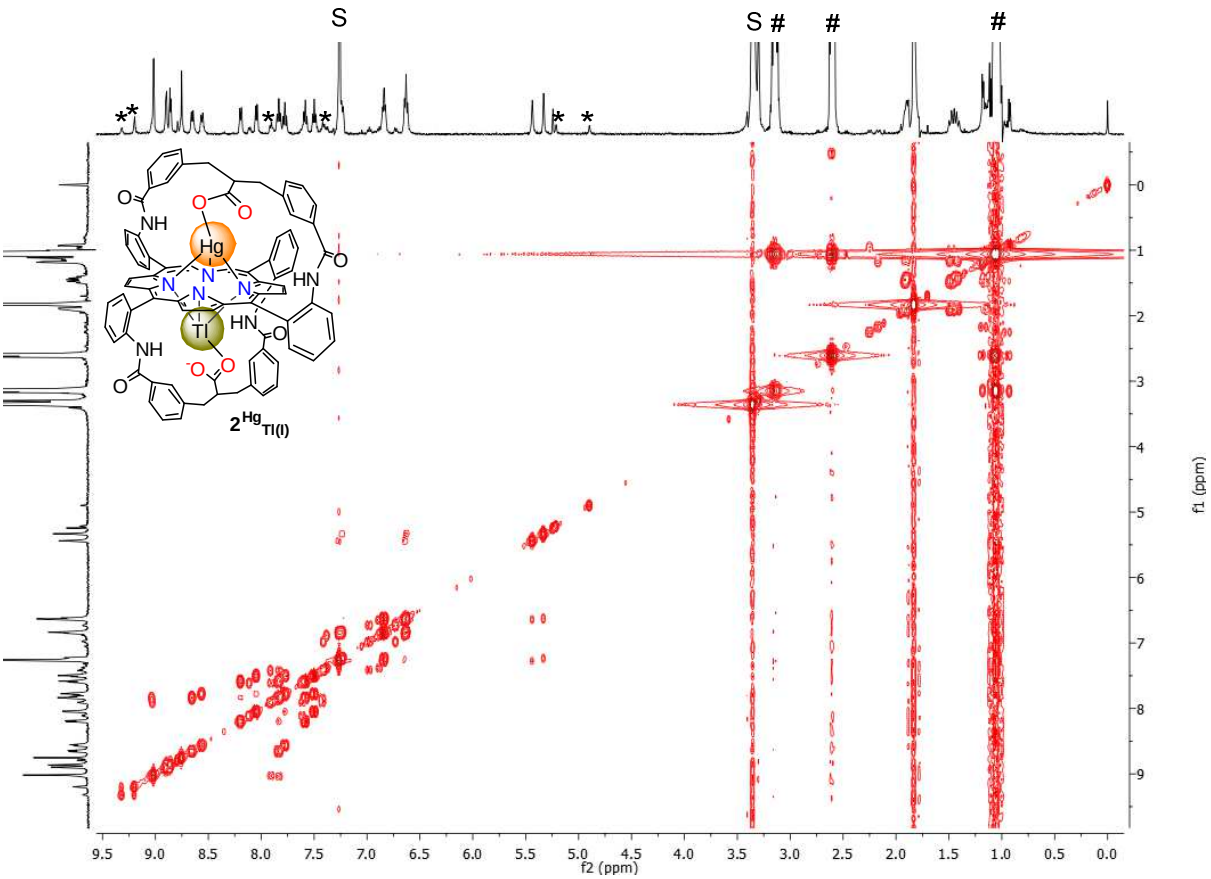

Figure S6. 2D COSY NMR spectrum of $\mathbf{2}^{Hg}_{Tl(I)}$ in $CDCl_3/CD_3OD$ (9:1) with 10 equiv. of DIPEA at 298 K (500 MHz). S = solvents, # = DIPEA, * = trace of the bimetallic complex $\mathbf{2Hg_2}$.[4]

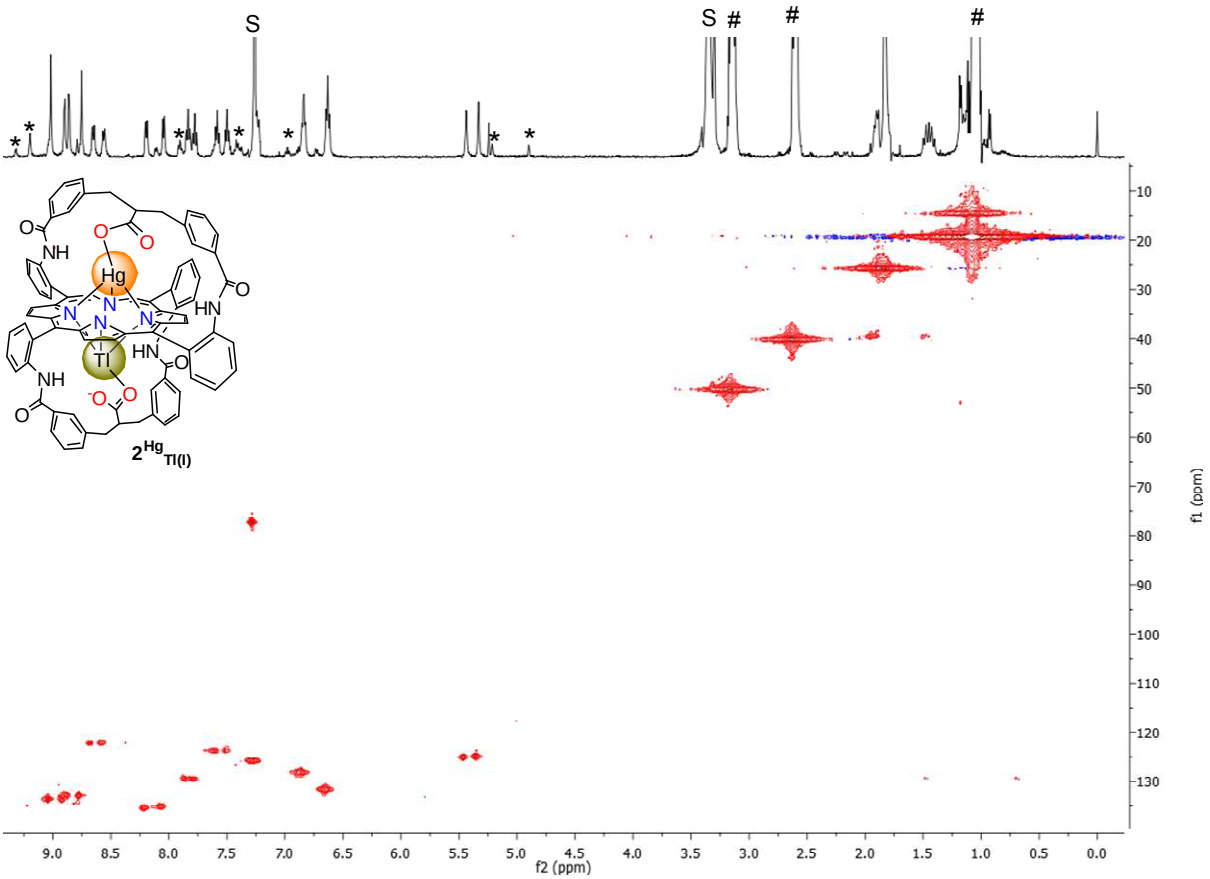

Figure S7. 2D HSQC NMR spectrum of $\mathbf{2}^{Hg}_{Tl(I)}$ in $CDCl_3/CD_3OD$ (9:1) with 10 equiv. of DIPEA at 298 K (500 MHz). S = solvents, # = DIPEA, * = trace of the bimetallic complex $\mathbf{2Hg_2}$.[4]

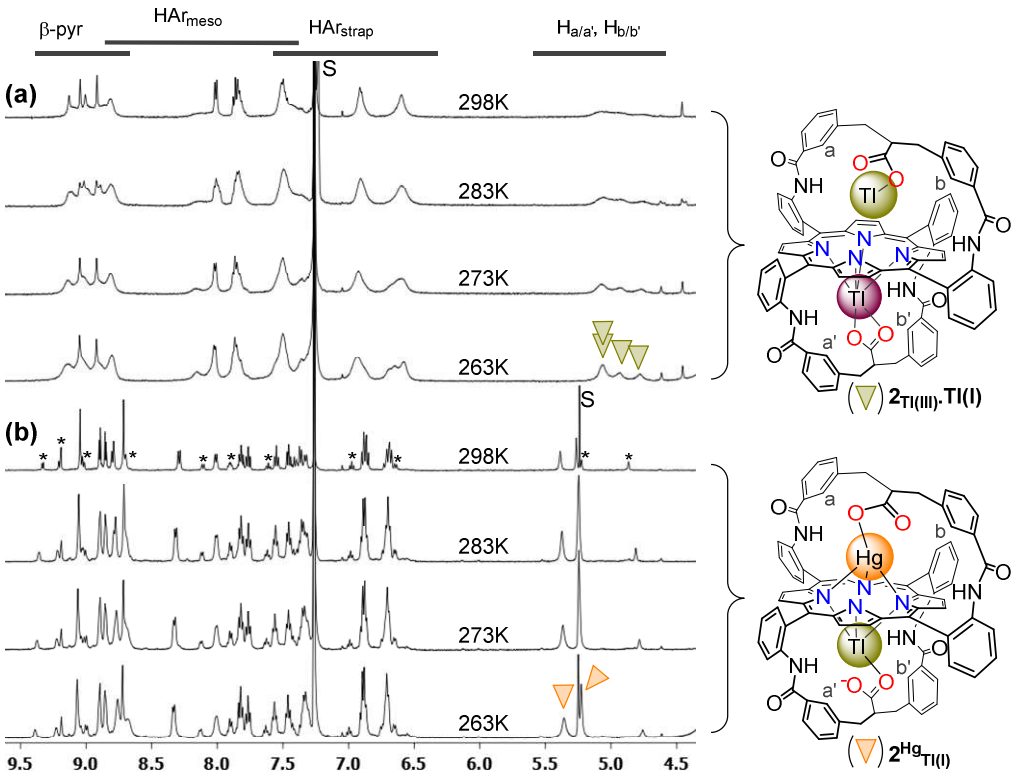

Figure S8. Comparison of the variable temperature ^{1}H NMR profiles of (a) **2$_{Tl(III)}$.Tl(I)** (disymmetric at 263 K) and (b) **2$^{Hg}_{Tl(I)}$** (C_2-symmetric at 263 K); conditions: $CDCl_3/CD_3OD$ (9:1), 10 equiv. of DIPEA, 500 MHz. S = solvents, * = trace of the bimetallic complex **2Hg$_2$**.[4]

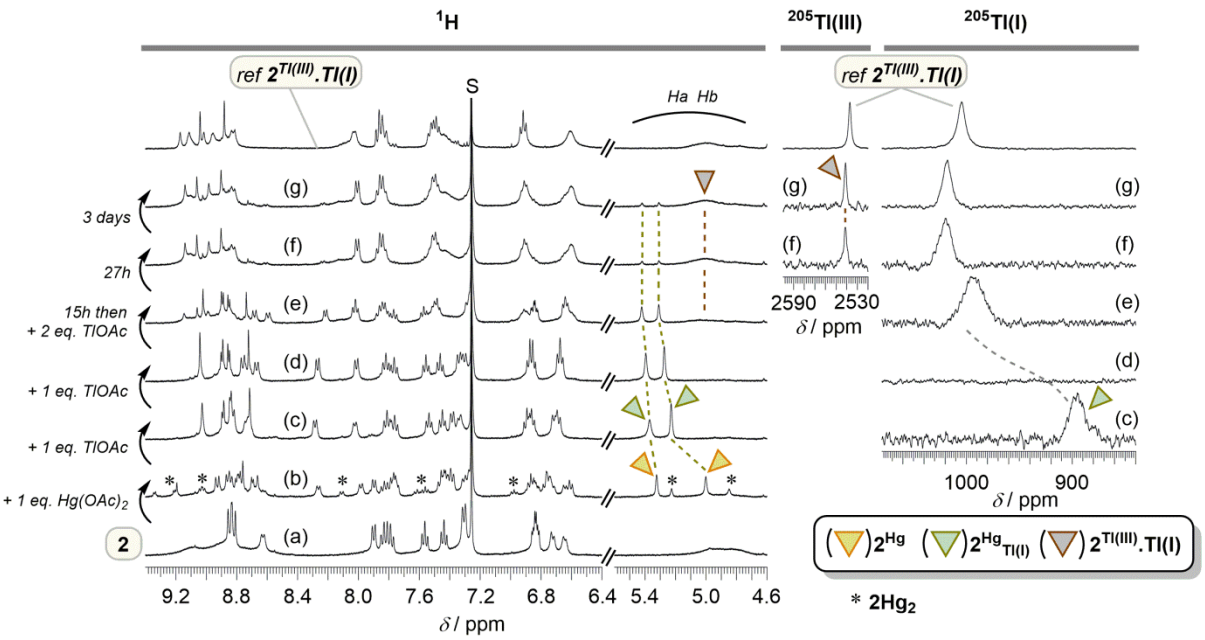

Figure S9. Formation and spontaneous evolution of $\mathbf{2}^{Hg}_{Tl(I)}$ monitored by ^{1}H and ^{205}Tl NMR spectroscopy ($CDCl_3/CD_3OD$ 9:1, 10 equiv. of DIPEA). $\mathbf{2}^{Hg}_{Tl(I)}$ was formed by the successive additions of $Hg(OAc)_2$ (a-b) and TlOAc (b-e), and was then allowed to stand in dark up to three days (d-g). S = solvent.

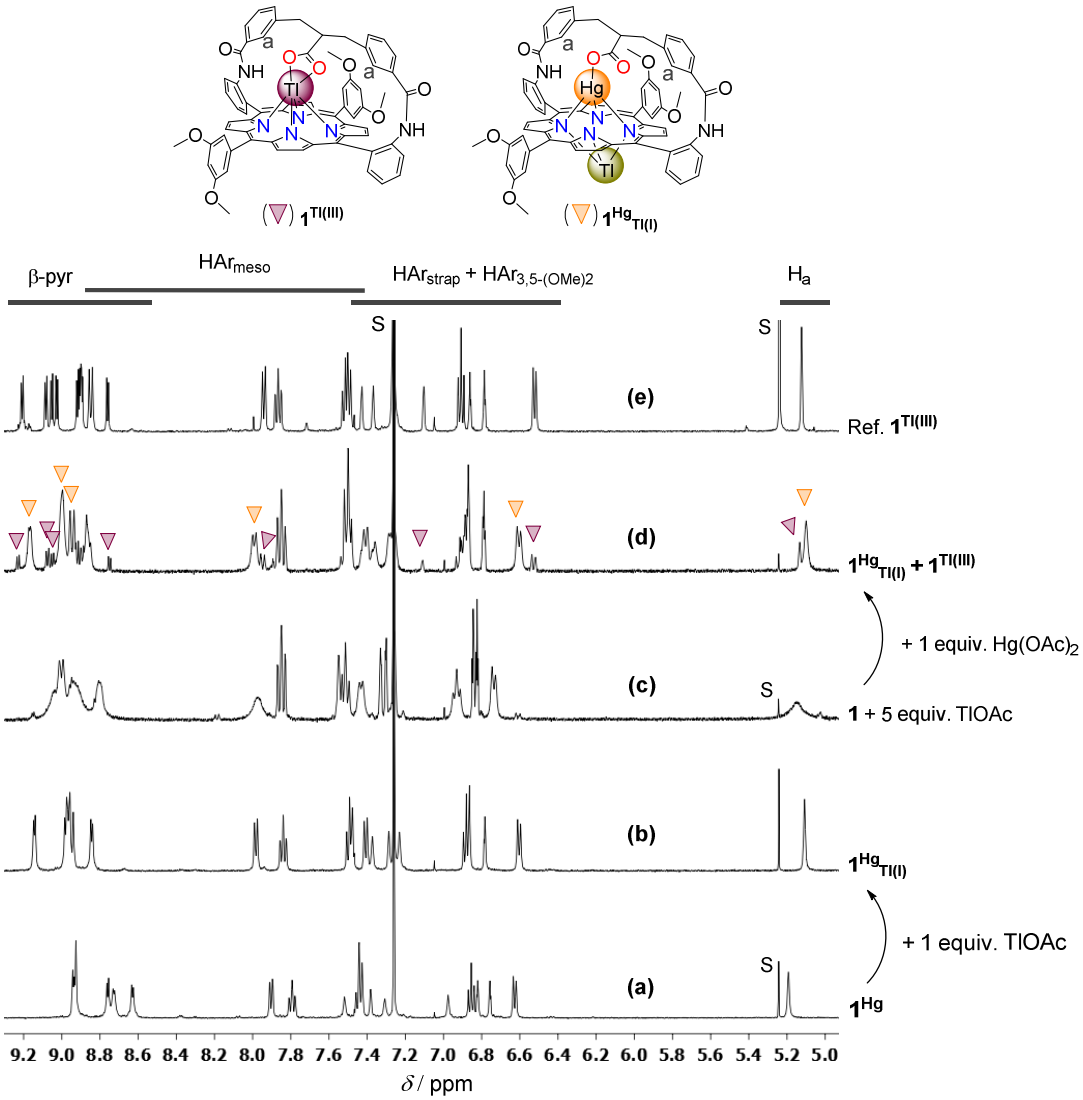

Figure S10. Influence of the order of introduction of TlOAc and $Hg(OAc)_2$ on the formation of $\mathbf{1}^{Hg}_{Tl(I)}$ monitored by ^{1}H NMR spectroscopy: (a-b) spectrum of $\mathbf{1}^{Hg}_{Tl(I)}$ obtained with a high selectivity by the successive addition of 1 equiv. of $Hg(OAc)_2$ and 1 equiv. of TlOAc to **1**; (c-d) spectra recorded after the successive addition of 5 equiv. of TlOAc and 1 equiv. of $Hg(OAc)_2$ to **1**, showing the presence of $\mathbf{1}^{Hg}_{Tl(I)}$ and $\mathbf{1}^{Tl(III)}$ in a *ca.* 5:1 initial ratio; e) spectrum of $\mathbf{1}^{Tl(III)}$ obtained by the addition of 1 equiv. of $Tl(OAc)_3$ to **1**. Conditions: 400 MHz, $CDCl_3/CD_3OD$ (9:1), 10 equiv. DIPEA, 298 K, obscurity. S = solvents.

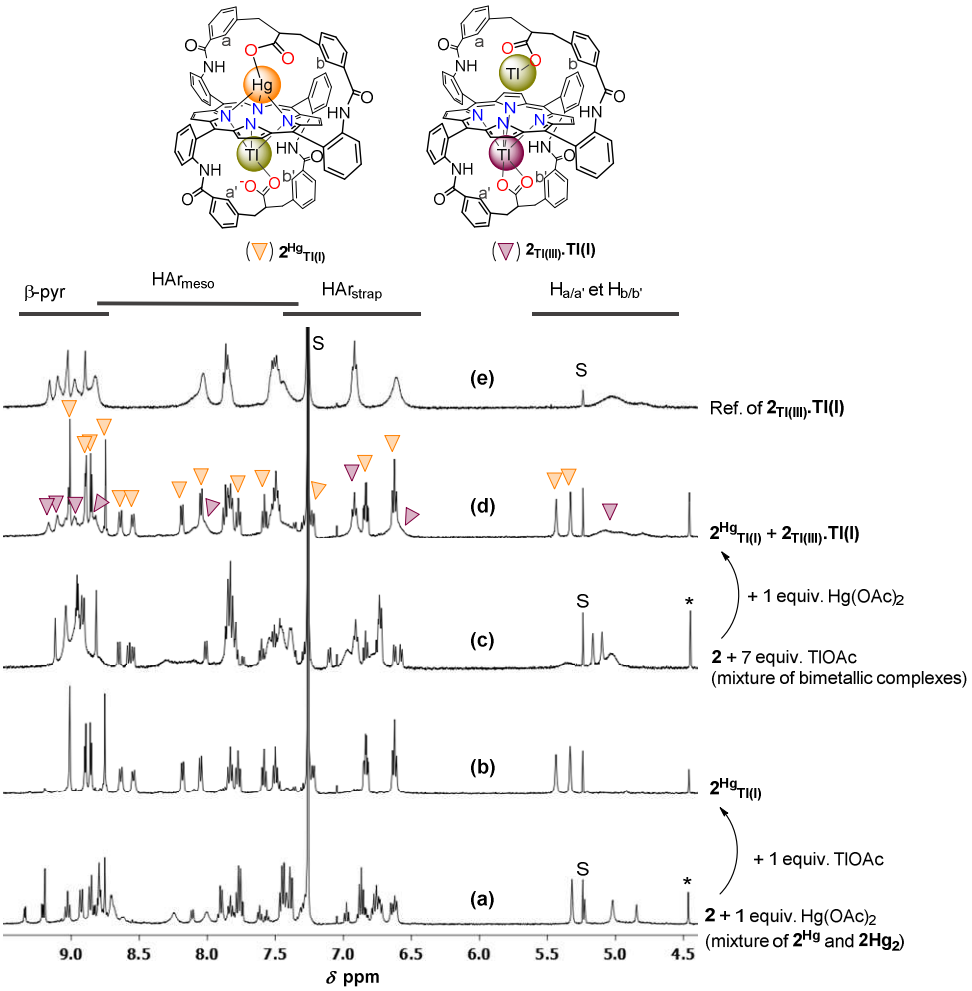

Figure S11. Influence of the order of introduction of TlOAc and $Hg(OAc)_2$ on the formation of $\mathbf{2}^{Hg}_{Tl(I)}$ monitored by ^1H NMR spectroscopy: (a-b) spectrum of $\mathbf{2}^{Hg}_{Tl(I)}$ obtained with a high selectivity by the successive addition of 1 equiv. of $Hg(OAc)_2$ and 1 equiv. of TlOAc to **2**; (c-d) spectra recorded after the successive addition of 7 equiv. of TlOAc and 1 equiv. of $Hg(OAc)_2$ to **2** showing, together with $\mathbf{2}^{Hg}_{Tl(I)}$, the presence of $\mathbf{2}_{Tl(III)}$**.Tl(I)** in a significant amount; (e) ^1H NMR spectrum of $\mathbf{2}_{Tl(III)}$**.Tl(I)** obtained by the addition of 1 equiv. of $Tl(OAc)_3$ and 7 equiv. of TlOAc to **2**.[9] Conditions: 500 MHz, $CDCl_3/CD_3OD$ (9:1), 10 equiv. DIPEA, 298 K, obscurity. S = solvents, * = impurity.

[9] V. Ndoyom, L. Fusaro, V. Dorcet, B. Boitrel and S. Le Gac, *Angew. Chem. Int. Ed.,* 2015, **54**, 3806-3811.

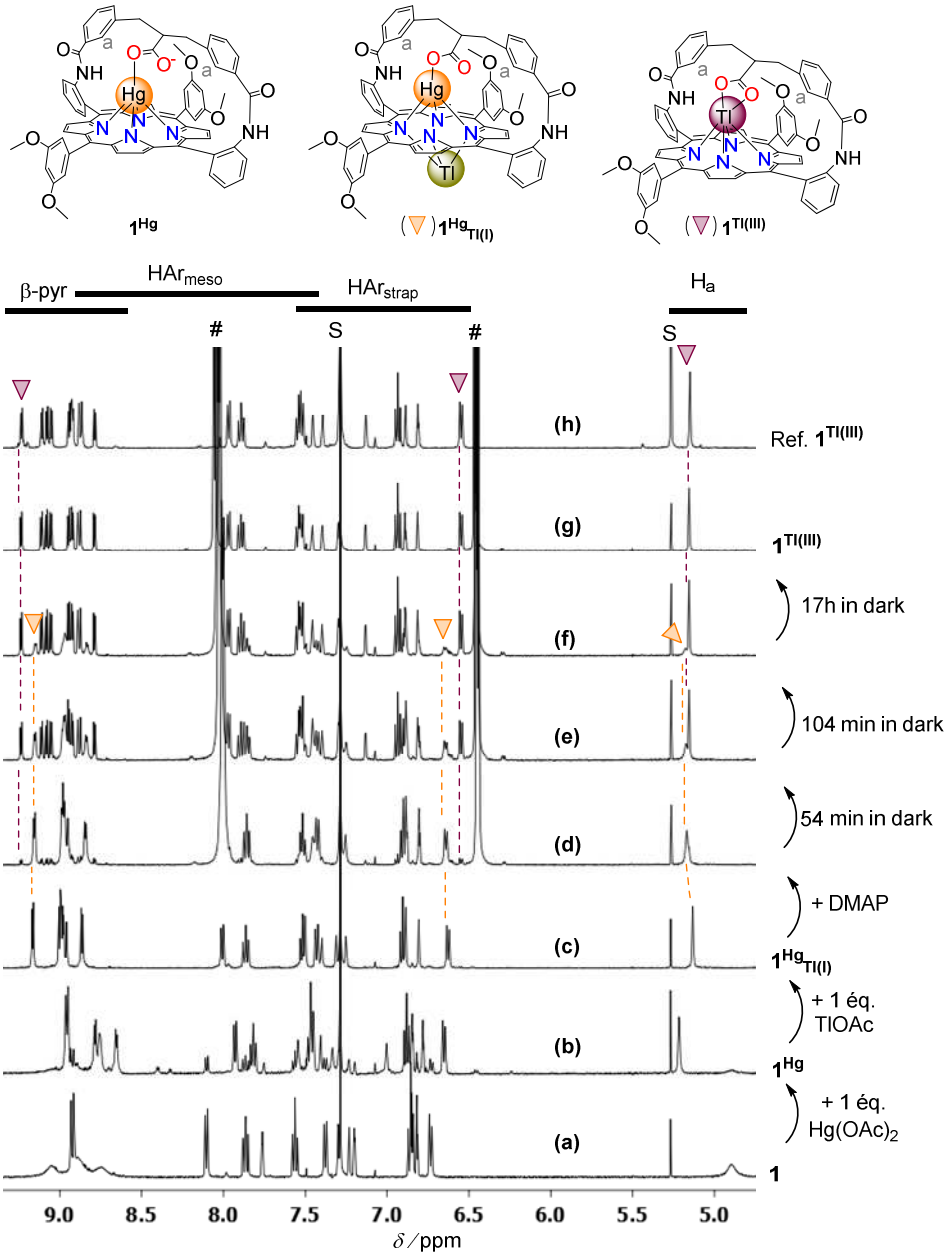

Figure S12. ^{1}H NMR monitoring of the spontaneous transformation $\mathbf{1}^{Hg}_{Tl(I)}$ -> $\mathbf{1}^{Tl(III)}$ in the presence of 11 equiv. of DMAP (d-g); (h) ^{1}H NMR spectrum of $\mathbf{1}^{Tl(III)}$ obtained by the addition of 1.5 equiv. of $Tl(OAc)_3$ to **1**. Conditions: 500 MHz, $CDCl_3/CD_3OD$ (9:1), 10 equiv. DIPEA, obscurity, 298 K. S = solvents, # = DMAP.

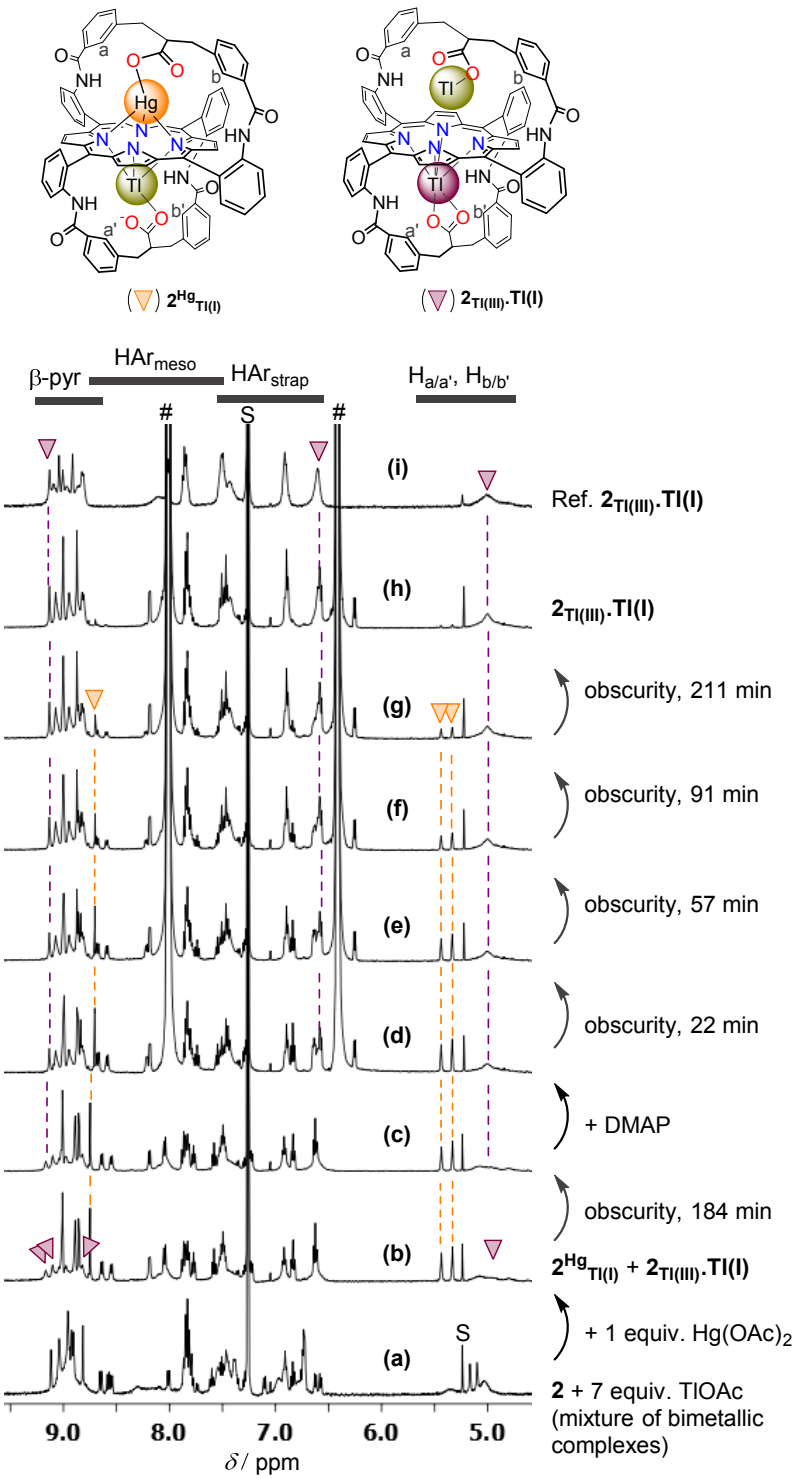

Figure S13. ^{1}H NMR monitoring of the spontaneous transformation $\mathbf{2}^{Hg}_{Tl(I)}$ -> $\mathbf{2}_{Tl(III)}$**.Tl(I)** without (b-c) or with 80 equiv. of DMAP (d-h); (i) ^{1}H NMR spectrum of $\mathbf{2}_{Tl(III)}$**.Tl(I)** obtained by the addition of 1 equiv. of $Tl(OAc)_3$ and 7 equiv. of TlOAc to **2**.[9] Conditions: 500 MHz, $CDCl_3/CD_3OD$ (9:1), 10 equiv. DIPEA, 298 K, obscurity. S = solvents, # = DMAP.

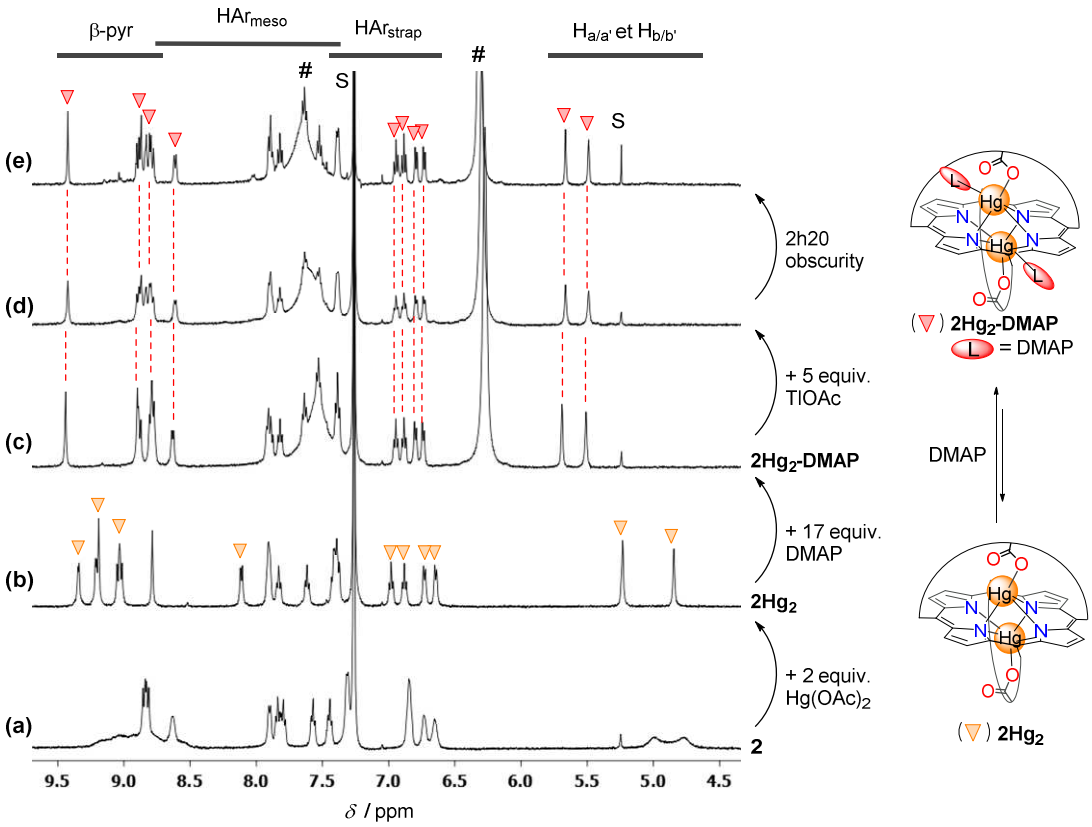

Figure S14. ^{1}H NMR experiment related to the Tl(I)-to-Tl(III) oxidation process, attempted with an excess of $Hg(OAc)_2$: (a-c) ^{1}H NMR spectra of the bimetallic complexes **2Hg$_2$** and **2Hg$_2$-DMAP** formed by the successive addition of 2 equiv. of $Hg(OAc)_2$ and 17 equiv. of DMAP to **2**;[4] absence of evolution of the solution upon the further addition of 5 equiv. of TlOAc (d-e). Conditions: 500 MHz, $CDCl_3/CD_3OD$ (9:1), 10 equiv. DIPEA, 298 K, obscurity. S = solvents, # = DMAP.

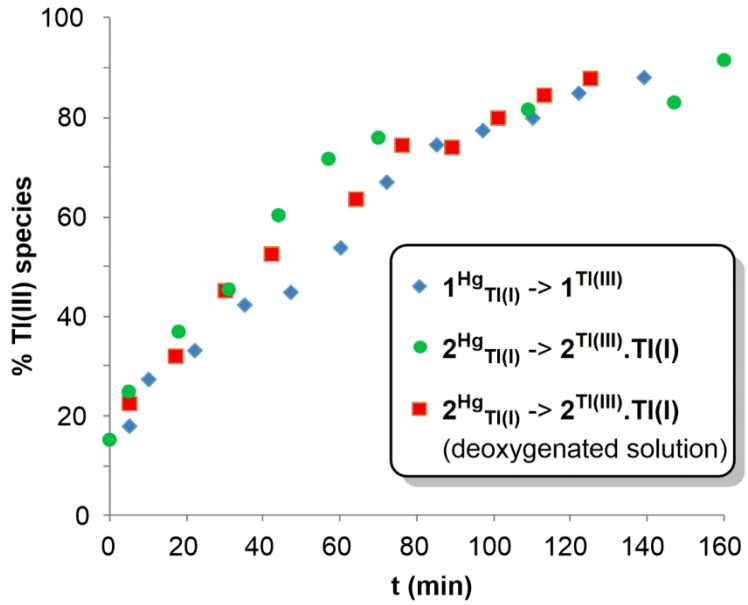

Figure S15. ^{1}H NMR monitoring of the transformations $\mathbf{1}^{Hg}_{Tl(I)} \rightarrow \mathbf{1}^{Tl(III)}$ and $\mathbf{2}^{Hg}_{Tl(I)} \rightarrow \mathbf{2}_{Tl(III)}\mathbf{.Tl(I)}$ carried out at ambient atmosphere or in deoxygenated solvents. Conditions: 500 MHz, $CDCl_3/CD_3OD$ (9:1), 10 equiv. DIPEA, *ca.* 35 equiv. DMAP, 298 K, obscurity. The percentages of Tl(III) species were determined from integration of appropriate signals *vs.* an internal reference (error ± 5 %).

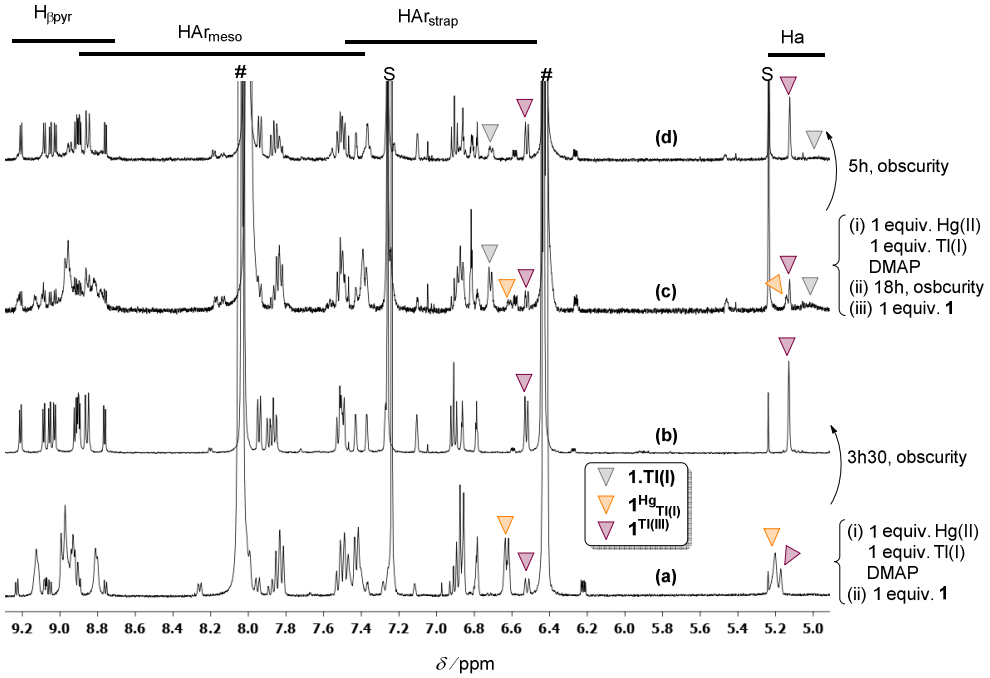

Figure S16. ^{1}H NMR experiments related to the Tl(I)-to-Tl(III) oxidation process attempted without porphyrin (c-d) (a-b is a reference experiment). Conditions: 500 MHz, $CDCl_3/CD_3OD$ (9:1), 10 equiv. DIPEA, 298 K, obscurity. S = solvents, # = DMAP.

(a-b) The successive addition of $Hg(OAc)_2$, TlOAc, DMAP and **1**, led to spectrum (a) recorded immediately. A *ca.* 5:1 initial ratio of $\mathbf{1}^{Hg}_{Tl(I)}$ and $\mathbf{1}^{Tl(III)}$ is observed (see text and Figure S10). Upon standing 3h30 in dark, $\mathbf{1}^{Tl(III)}$ is obtained quantitatively (b).

(c-d) The successive addition of $Hg(OAc)_2$, TlOAc and DMAP led, upon standing 18h in dark and subsequent addition of **1**, to spectrum (c), showing that **1.Tl(I)** is the major species while $\mathbf{1}^{Tl(III)}$ is the minor one. $\mathbf{1}^{Tl(III)}$ is likely formed when **1** is added and not during the 18 hours in the absence of **1** (deduced from comparison with spectrum (a)); spectrum (d) was recorded upon standing 5h in dark, showing $\mathbf{1}^{Tl(III)}$ as a major species.

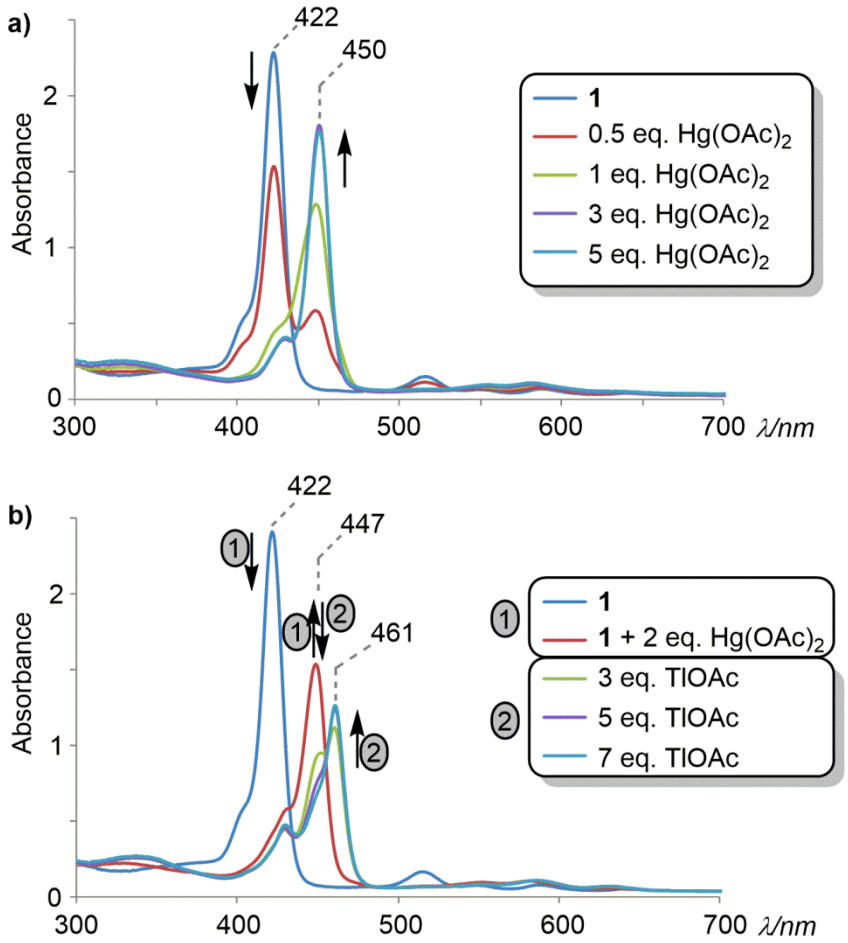

Figure S17. Monitoring of the metallation of **1** with Hg(II) and Tl(I) by UV-vis absorption spectroscopy: (a) titration of **1** with $Hg(OAc)_2$ (the Soret band at 450 nm corresponds to dinuclear species, see ref [4] and [10]); (b) successive addition of $Hg(OAc)_2$ and TlOAc to **1**. Conditions: $CHCl_3/CH_3OH$ (9:1), 10 equiv. DIPEA, obscurity.

[10] (a) M. F. Hudson and K. M. Smith, *Tetrahedron Lett.,* 1974, **26**, 2223-2226; (b) M. F. Hudson and K. M. Smith, *Tetrahedron Lett.,* 1974, **26**, 2227-2230.

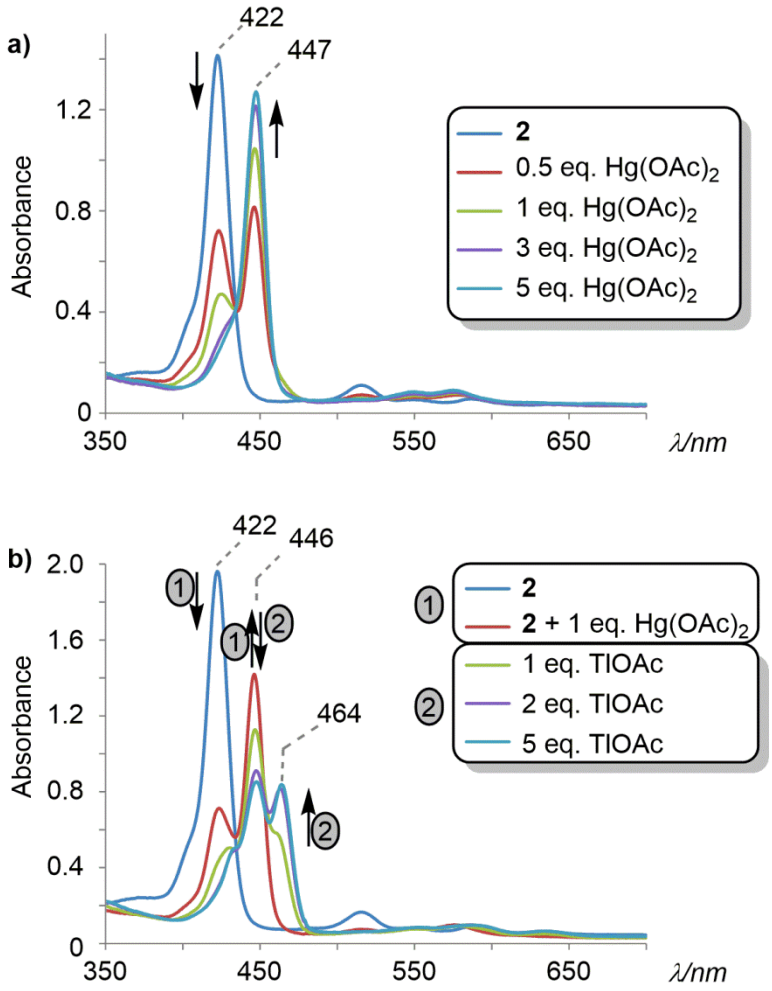

Figure S18. Monitoring of the metallation of **2** with Hg(II) and Tl(I) by UV-vis absorption spectroscopy: (a) titration of **2** with $Hg(OAc)_2$ (the Soret band at 447 nm corresponds to dinuclear species, see ref [4] and [10]); (b) successive addition of $Hg(OAc)_2$ and TlOAc to **2**. Conditions: $CHCl_3/CH_3OH$ (9:1), 10 equiv. DIPEA, obscurity.

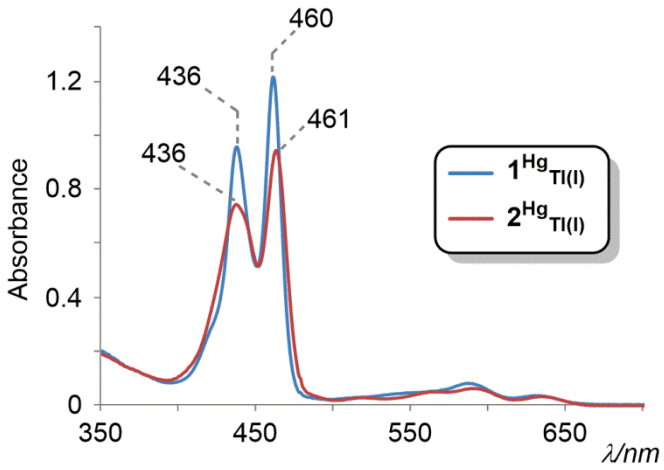

Figure S19. UV-vis absorption spectra of $\mathbf{1}^{Hg}_{Tl(I)}$ and $\mathbf{2}^{Hg}_{Tl(I)}$ obtained from a 1/500 dilution of NMR tube solutions containing exclusively these complexes. In both cases, an intense Soret band at 436 nm is observed, evidencing the formation of the corresponding Tl(III) species [$\mathbf{1}^{Tl(III)}$ and $\mathbf{2}_{Tl(III)}$**.Tl(I)**] upon dilution. Conditions : $CHCl_3/CH_3OH$ (9:1), 10 equiv. DIPEA, obscurity.